On three-axis attitude control strategy with its application to 3D orbital maneuvers considering overactuated space systems

A.H. Mazinan[1] and A. Shirazi[2]

[1]Department of Electrical Engineering, Azad University, Tehran, Iran
mazinan@azad.ac.ir
[2]Department of Aerospace Engineering, Ryerson University, 350 Victoria Street, Toronto, Ontario, Canada M5B 2K3

Abstract

With the development of space technology, 3D orbital maneuvers are taken into real consideration as a challenging issue. The approach proposed here is organized to deal with a number of overactuated space systems via hybrid multi-purpose three-axis attitude control strategy. In a word, the control idea attempts to address a new autonomous approach, in order to deal with orbital maneuvers in a wide range of spacecraft parameters variation along with trajectory optimization. This control approach is organized to handle two sets of low-high thrusters, while pulse-width pulse-frequency modulator as well as control allocation are employed to track three-axis referenced rotational commands that are directly related to steering angles. The main contribution of the approach presented here is to propose an applicable control strategy to be able to deal with the orbital transferring process, while most of the parameters of spacecraft as well as the space environments are taken into real consideration.

1. Introduction

The present research is organized to deal with overactuated spacecrafts in a wide range of parameters variations to be applicable in the process of 3D orbital maneuvers, while time history of the orbital parameters are exploited. The present orbital parameters including semi major axis, eccentricity, apogee radius, inclination, argument of perigee and right ascension of ascending node are dealt with to present steering angles in the form of quantic polynomials. It is noted that the proposed control approach is realized to track three-axis referenced rotational angles that are directly generated from quantic polynomials steering angles by considering the whole of the spacecraft parameters including variation of the central mass, variation of the moments of inertial, thrust vector misalignments, thrust vector disturbances, propellant engine arms, thrusters dynamics and so on to be efficient and accurate. In the approach proposed here, the orbital maneuvers as one of the main issues in conceptual and preliminary design of spacecrafts, in different space missions, are handled through solving an optimization problem. The main issue in such optimizations is that the common algorithms such as genetic algorithm and simulated annealing algorithm are not effectual in finding optimal transfer, as long as they are purely used in optimization. This research presents an approach to optimize high-thrust orbit transfers using modified evolutionary algorithm, where a hybrid three-axis autonomous attitude control strategy, namely TAAC is realized to deal with a kind of spacecraft entitled upper-stage system. In this regards, the control strategy plays an important role in the process of 3D orbital transferring in finite burn in line with the referenced steering angles commands, generated through guidance system. Despite low-thrust transfers along with low acceleration and thrust to weight ratios, high-thrust orbital maneuvers require large amount of thrust magnitude. It is shown that two sets of thrusters need to be handled through the control strategy realization, where the first one is related to high thrusts in the y and z axes and also second one is related to a number of further low thrusts that are related x-axis. There are currently a set of pulse-width pulse-frequencies (PWPFs) and control allocations (CAs), while PWPF modulators are employed to be able to handle on-off high-low thrusters and CA is realized to assist in the process of coping with a kind of overactuated spacecraft entitled upper-stage system.

Regarding the background in the area of system presented, it should be noted that during the past decades, a number of efficient and applicable studies on the spacecraft attitude control have been carried out that are discussed in the proceeding paragraphs. Moreover, concerning the recent potential research in the area of the trajectory optimization, Curtis et al. present the initial information regarding the orbital mechanics that are so useful to consider the orbital maneuvers, at first [1]. Trajectory optimization is revealed regarding the continuous-thrust spacecraft round trip flights through pseudo spectral method. The movement of the spacecraft is discussed through the Gauss equation via the modified equinoctial elements in the Gauss orbital coordinates [2]. Yam et al. present constrained global optimization regarding the low-thrust interplanetary trajectories, where the Sims-Flanagan transcription method is used to produce the nonlinear programming problem [3]. Xiao-yong et al. propose an approach based on virtual gravitational body for low-thrust trajectory optimization, while the original optimal control problem is converted into a nonlinear programming problem that could be solved fast owing to the analytical nature of conic arcs [4]. There are some investigations to be considered [5]-[8].

Concerning the recent potential research in the area of spacecraft control, Pieper et al. presents error analysis of direction cosines and quaternion parameters techniques regarding aircraft attitude determination, while Lovren et al. presents strapdown inertial navigation system for the flat-Earth model [9]-[10]. Xiao et al. present the attitude stabilization for spacecrafts with actuator saturation and partial loss of control effectiveness, while the attitude system that is represented by modified Rodriguez parameters is considered in the presence of external disturbances, actuator saturation and uncertain inertia parameters [11]. There are also some investigations to be considered [12]-[15]. Finally, there are two benchmarks [16]-[17] to be compared along with the proposed approach performance. The rest of the manuscript is organized as follows: The guidance approach is presented in Section 2. The proposed TAAC control strategy is given in Section 3, while the simulation results are then given in Section 4. Finally, the research concludes the outcomes in Section 5.

2. The guidance approach

2.1. The dynamics

Let $\vec{r}$ denotes the position vector of the vehicle that is related to the Earth. The acceleration of the spacecraft relative to the planet, $\dot{\vec{v}}$, evaluated in the coordinate system x, y, z assuming a non-Keplerian motion that can be written as

$$\dot{\vec{r}} = \vec{v}$$
$$\dot{\vec{v}} = -\mu.\vec{r}/r^3 + T.\vec{n}/m \qquad (1)$$
$$\dot{m} = T/v_e$$

where $\vec{r}$ and $\vec{v}$ denote the spacecraft position and velocity vectors, respectively, and the scalar r denotes the magnitude of radius vectors that is taken as $r = |\vec{r}|$. Here, $\vec{n}$ is taken as the normalized vector of thrust direction relative to the inertial reference frame and T is taken as the magnitude of thrust with respect to motor performance. Furthermore, m is taken as the spacecraft mass, where the constant μ denotes the central body's gravitational constant and v_e represents the exhaust velocity, which can be stated as the function of specific impulse of propellant and the Earth's gravitational acceleration as $v_e = I_{sp}.g_0$. By considering 3D motion of spacecraft between space orbits, thrust direction can be stated as follows

$$\vec{n} = \begin{bmatrix} \cos(\alpha)\cos(\beta) \\ \cos(\alpha)\sin(\beta) \\ \sin(\alpha) \end{bmatrix} \qquad (2)$$

Here, α and β are taken as the thrust direction angles. It is noted that these thrust steering angles are measured with respect to inertial coordinate system. In addition to derivation of state vectors, it is necessary to calculate orbital parameters in each time step, in order to evaluate the shape and orientation of space orbit. Thrust direction angles in ignition segment need to be specified so that the optimal transfer can be achieved.

2.2. The optimization approach

In order to optimize a transfer trajectory, a scalar cost function has to be defined to measure the trajectory's merit. Since the transfer is not coplanar, both the shape and orientation of final orbit is considered as the target in optimization. Therefore, the goal is to maximize the accuracy of final orbits in this transferring process with respect to provided thrust profile. Considering t_f as the total burn time in orbit transfer, the cost function may be defined as

$$J = \left(\frac{a(t_f) - a_{des}}{\sigma_a}\right)^2 + \left(\frac{e(t_f) - e_{des}}{\sigma_e}\right)^2 + \left(\frac{i(t_f) - i_{des}}{\sigma_i}\right)^2 + \left(\frac{\omega(t_f) - \omega_{des}}{\sigma_\omega}\right)^2 + \left(\frac{\Omega(t_f) - \Omega_{des}}{\sigma_\Omega}\right)^2 \qquad (3)$$

where a, e, i, ω and Ω denote the semi-major axis, eccentricity, inclination, argument of perigee and right ascension of ascending node at the end of orbit transfer, respectively. Similarly, a_{des}, e_{des}, i_{des}, ω_{des} and Ω_{des} represent the desired values of related parameters at the end of orbit transfer. Moreover, σ_a, σ_e, σ_i, σ_ω and σ_Ω are taken as weighting coefficients that are related to each one of the parameters, which are specified based on desired accuracy according to mission objective.

This definition of cost function fairly scales the weighting coefficients. As based on this definition, if $J < 1$, all of the parameters at the end of orbit transfer reach the desired values with acceptable accuracies. The variation of thrust direction angles are to be specified by the guidance law so that the performance index can be defined by Eq. (3) to become minimal. The guidance commands are initially assumed as the polynomial functions of time as

$$\alpha(t) = \sum_{i=0}^{n} a_i t^i \qquad (4)$$

$$\beta(t) = \sum_{i=0}^{n} b_i t^i \qquad (5)$$

where t represents the time that starts with the ignition of engine rocket, a_i and b_i are taken as the polynomial coefficients of direction angles and finally n is taken as the degree of polynomials. The optimal values of coefficients that result the best transfer accuracy are achieved using intelligent search methods. The methods such as the genetic algorithm (GA) use neither sensitivity derivatives nor reasonable starting solutions, particularly. In this evolutionary algorithm that is based on natural evolution concept, the natural selection increases the surviving capabilities of a population over the generations. The genetic information of each individual is stored in a chromosomal string and the goodness of individual is measured by defining a fitness function based on the string. Only the individuals with better characteristics survive during the evolutionary process so that the fitness function can be minimized. The GA begins with no knowledge of how to design an optimal transfer trajectory and evolves to near optimal solution.

2.3. The mission objective

The problem of guidance optimization in high-thrust transfers is considered in which all of the orbital elements can change during the orbital maneuvers. Table 1 tabulates the characteristics of initial and final orbits in the present space mission.

Table 1. The orbital parameters regarding the initial and the final trajectories.

The parameters	The initial orbit	The final orbit
Eccentricity (e)	0.3	0.4
Semi-major axis (a)	18e3 km	2e4 km
Inclination (i)	50^o	60^o

Argument of perigee (ω)	40^o	13.13^o
Right ascension of ascending node (Ω)	10^o	33.7^o

Regarding Table 1, the illustration of space orbits is correspondingly depicted in Fig. 1. The intersection of the initial and the final orbits occurs at $\vec{r}_0 = 3015\hat{i} + 8506\hat{j} + 9359\hat{k}\ km$. This radius is related to true anomalies of 30^o and 43.09^o in initial orbit and final orbits, respectively. The spacecraft dry mass, thrust magnitude and specific impulse are considered in Table 2 for the present transferring process, as well.

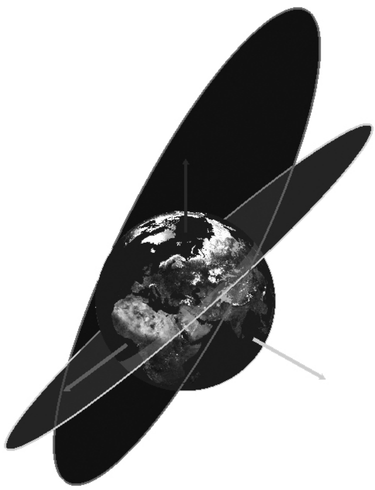

Fig. 1. The 3D visualization of the proposed mission orbits.

It is expected that the orbit transfer has the error of 100 km and 0.01 in semi-major axis and eccentricity, respectively. Also, the desired accuracy for orbital orientation angles including inclination, argument of perigee and right ascension of ascending node are assumed to be 0.1 deg.

Table 2. The orbit transfer specifications.

The parameters	The values
Dry mass (m_0)	500 kg
Thrust (F)	9.035 kN
Specific impulse (I_{sp})	282 s
Burn time (t_b)	37.86

2.4. The optimal orbit transfer

The high-thrust orbit transferring in the proposed mission is optimized using the GA. Regarding the impulsive assumption, the burn should start at true anomaly of $\theta_0 = 30^\circ$ in initial orbit. However, the optimal starting position of burn arc is unknown, since the high thrust approach is employed in current concept. While the optimal starting position in these two concepts has little differences, initial boundary that limits in the span of $25 < \theta_0 < 35$ for true anomaly is considered in order to avoid confronting large domain of undesirable answers. The optimization is carried out using the GA based on different degree of polynomials for steering angles. With respect to desired accuracies, defined in mission objective, the required polynomial for satisfying the proposed cost function ($J < 1$) is quantic and the minimum degree of polynomial for achieving acceptable accuracy is taken as $n = 5$.

3. The proposed TAAC control strategy

3.1. The spacecraft dynamics

The attitude dynamic equation is organized based on the following formula

$$\boldsymbol{\tau_c} = \frac{d\boldsymbol{H_c}}{dt} + \boldsymbol{\omega} \times \boldsymbol{H_c} \tag{6}$$

where $\boldsymbol{\tau_c}$ denotes three-axis control torques, $\boldsymbol{H_c}$ denotes angular momentum vector in the body coordinate contains H_μ and finally $\boldsymbol{\omega}$ denotes as angular velocity vector in the body coordinate contains ω_μ, $\mu = x, y, z$. Now, by addressing the three-axis angular velocities, the three-axis control torques of the spacecraft are realized as

$$\begin{cases} \tau_x = \dot{H}_x + \omega_y H_z - \omega_z H_y \\ \tau_y = \dot{H}_y + \omega_z H_x - \omega_x H_z \\ \tau_z = \dot{H}_z + \omega_x H_y - \omega_y H_x \end{cases} \tag{7}$$

Moreover, the attitude dynamic equations are easily resulted by

$$\begin{cases} \dot{\omega}_x = \dfrac{\tau_x}{I_x} - \dfrac{(I_z - I_y)}{I_x}\omega_y\omega_z \\ \dot{\omega}_y = \dfrac{\tau_y}{I_y} - \dfrac{(I_x - I_z)}{I_y}\omega_x\omega_z \\ \dot{\omega}_z = \dfrac{\tau_z}{I_z} \quad \dfrac{(I_y - I_x)}{I_z}\omega_x\omega_y \end{cases} \tag{8}$$

where $\boldsymbol{I}$ denotes three-axis moments of inertial matrix contains I_μ in the μ direction, $\mu = x, y, z$. Finally, by assuming $\times$ as cross product, the results can briefly be presented as $\boldsymbol{\tau_c} = \boldsymbol{I}\dot{\boldsymbol{\omega}} + \boldsymbol{\omega} \times \boldsymbol{I}\boldsymbol{\omega}$.

3.2. The strategy realization

The proposed control strategy is now illustrated in Fig. 2 that is based upon double closed loops including the inner and the corresponding outer loops in low and high thrust modes. The outer closed loops of the present strategy are organized to deal with the three-axis rotational angles, while the x-axis rotation is related to low thrust mode and the y and z-axis rotation are related to the high thrust mode, as well, regarding the spacecraft under control $(SPCFT)$. The responsibility of the both outer closed loops are to adjust the three-axis system rotational angles (SRA_{xyz}) to track the three-axis referenced rotational angles (RRA_{xyz}). Furthermore, the responsibility of the both inner closed loops are to adjust the three-axis system angular rates (SAR_{xyz}) to deal with the three-axis angular rate errors to be zero. In this approach, the four controllers are designed, while two of them including the x-axis rotational angles control in low thrust mode (RAC_{Lx}) and the y and z-axis rotational angles control in high thrust mode (RAC_{Hyz}) are designed in the outer closed loops. Hereinafter, the rest of them including the x-axis angular rate control in low thrust mode (ARC_{Lx}) and the y and z-axis angular rates control in high thrust mode (ARC_{Hyz}) are designed in the inner closed loops. It is noted that the RAC_{Lx} and RAC_{Hyz} are designed based upon the proportional-integral-derivative approach, while ARC_{Lx} and ARC_{Hyz} are designed based on the proportional approach.

Due to the fact that reaction control strategies do not possess the linear relationship between the input to the controller and its output torque, the pulse-width pulse-frequency ($PWPF$) modulators are needed to relate between the level of required torque and the width and the frequency of pulses, in order to shape the non-linear output of on-off thrusters into linear request output. Therefore, there are the traditional three-axis $PWPF$ modulators, while $PWPF_{Lx}$ is related to the low thrust mode and also $PWPF_{Hyz}$ is related to the high thrust mode.

4. The simulation Results

The simulation results in the proposed research are twofold. The first one is related to the process of orbital transferring and also the second one is related to the corresponding control approach. At first, it is needed to note that the specifications of the spacecraft considered in the present research are taken as the engine thrust's level regarding the propellant engine, the dry and the fuel mass, the initial three-axis rotational angles and finally the initial three-axis angular rates, presented by

$$T = 9.035kN$$
$$M_{fuel} = 644kg$$
$$M_{dry} = 500kg$$
$$\begin{bmatrix}\varphi_0\\ \theta_0\\ \psi_0\end{bmatrix} = \begin{bmatrix}0\\ -48.19\\ -66.98\end{bmatrix}\deg \tag{9}$$
$$\begin{bmatrix}\omega_x\\ \omega_y\\ \omega_z\end{bmatrix} = \begin{bmatrix}0\\ 0\\ 0\end{bmatrix}\frac{rad}{s}$$

Regarding the orbital transferring process, it should be noted that an optimal value of initial true anomaly is found as $\theta_0 = 29.46^\circ$ at the end of optimization, which results the initial conditions as $\vec{r}_0 = [3128\ \ 8490\ \ 9317]\,km$ and $\vec{v}_0 = [-5.8059\ \ 0.8454\ \ 2.1937]\,km/s$.

The polynomial coefficients that are calculated through optimization method are now tabulated in Table 3. The information presented here is to generate the steering angles suitable to acquire the orbital transferring process. Regarding the proposed control strategy, at first, the information regarding the steering angles need to be taken as the RRA in the three axes through Eqs. (4)-(5), while the tracking outcomes are depicted in Figs. 3 to 5, respectively.

The variation of the three axis cg in the process of approach simulation is illustrated in Fig. 6. It is obvious that the x-axis cg is varied with respect to time in the span of 0-0.1 m, where the y-axis cg is taken as 0.02 to be constant and the variation of the z-axis cg is ignored, i.e. it is taken to be zero. The three-axis EA are now illustrated in Fig. 7, while the variation of x-axis EA is only taken into consideration. It means that there are no variations in the y and z-axis EA. The thrust vector misalignments are shown in Fig. 8. As is obvious, the variations of α_d and β_d are the same and both of them are varied in the form of the two-level step signals, where at the beginning of the simulation, they are taken to be 0.5 degree and consequently are taken to be 0.25 degree, as well. It is apparent that at the beginning of the propellant engine performance the thrust vector misalignments are high with respect to its steady state, due to the fact that this factor plays an important role, initially. The three-axis thrust vectors with disturbances are presented in Fig. 9, while the three-axis torques disturbances are shown in Fig. 10. The variation of the moments of inertial are also presented in Fig. 11. Hereinafter, in an effort to make the investigated results in the comparable manner, the two potential benchmarks including the Yang and the Cai strategies, investigated in recent years, are now chosen to consider. Moreover, there are the following criteria to be considered in Table 4 including (1) the maximum three-axis RAE in steady state, (2) the maximum three-axis ARE in steady state, (3) the trajectory convergence time and finally (4) the number of enabling the sets of the thrusters, which are all important to evaluate the proposed approach performances w. r. t. the corresponding benchmarks. As a deduction matter, the results indicate that the proposed control approach is now well behaved in line with the present benchmarks regarding the items (1) and (2), while the Yang approach is well behaved regarding the item (3) w. r. t. the aforementioned approaches.

Table 3. The polynomial coefficients.

	$n = 5$
a_0	48.190811
b_0	-66.983250
a_1	-0.127846
b_1	3.315642
a_2	-0.081546
b_2	-0.461685
a_3	0.011748
b_3	0.025729
a_4	-0.000478
b_4	-0.000623
a_5	6.067e-6
b_5	5.525e-6

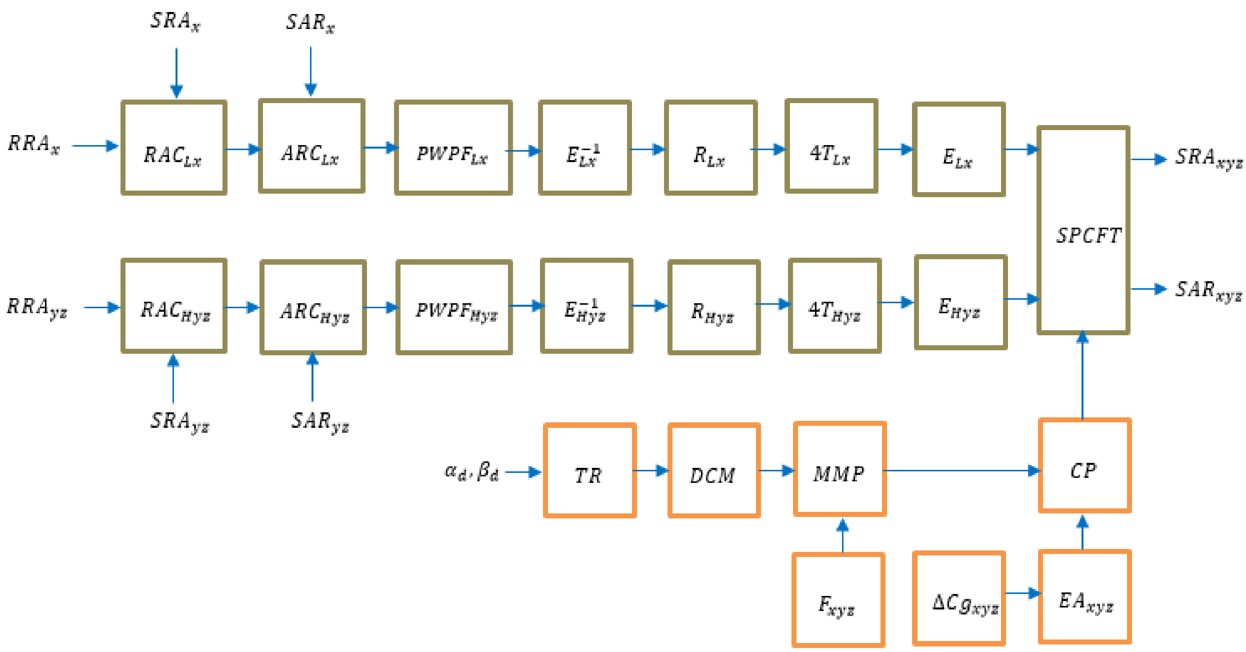

Fig. 2. The schematic diagram of the proposed TAAC control strategy.

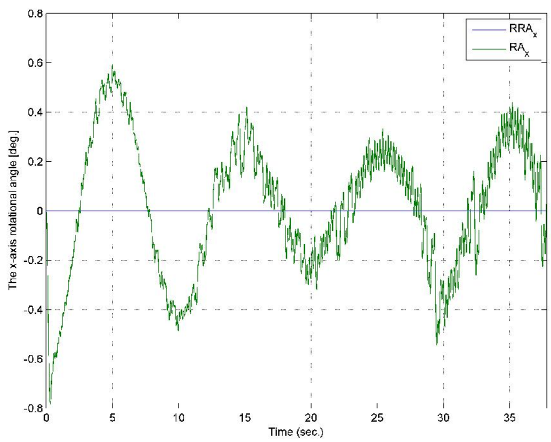

Fig. 3. The x-axis RRA tracking.

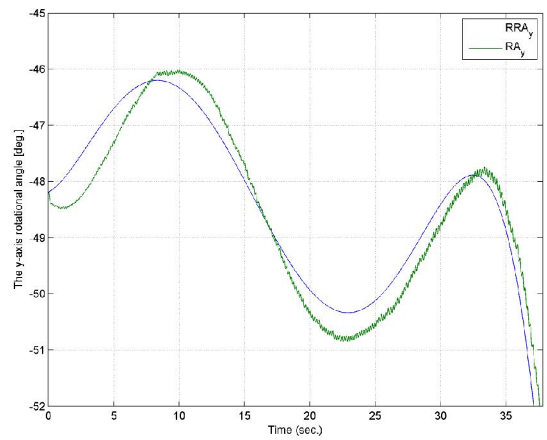

Fig. 4. The y-axis RRA tracking.

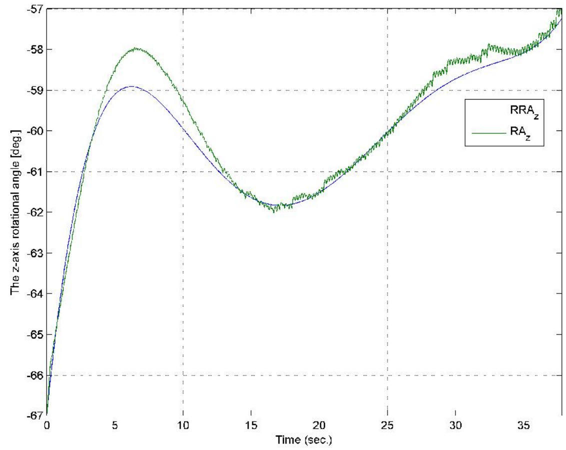

Fig. 5. The z-axis RRA tracking.

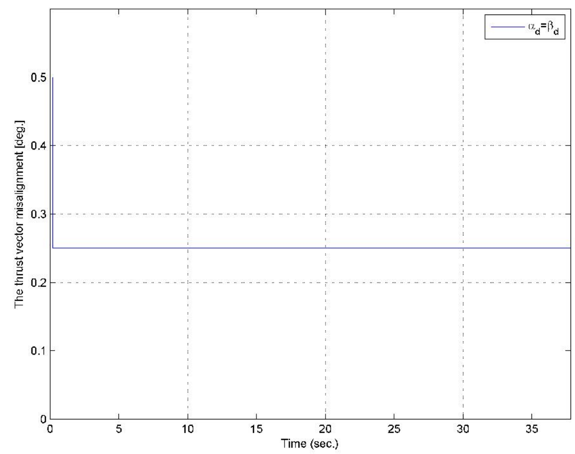

Fig. 8. The thrust vector misalignments.

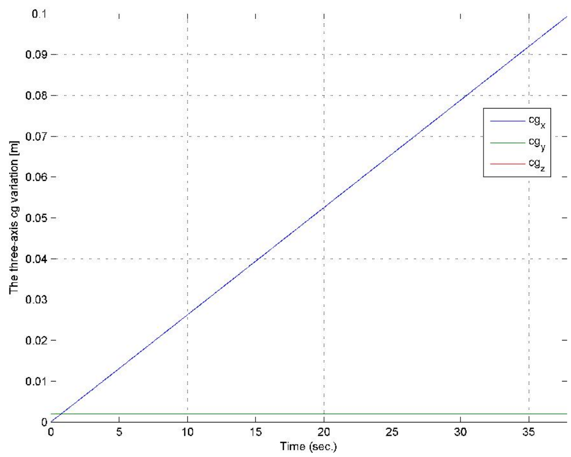

Fig. 6. The three axis cg variation.

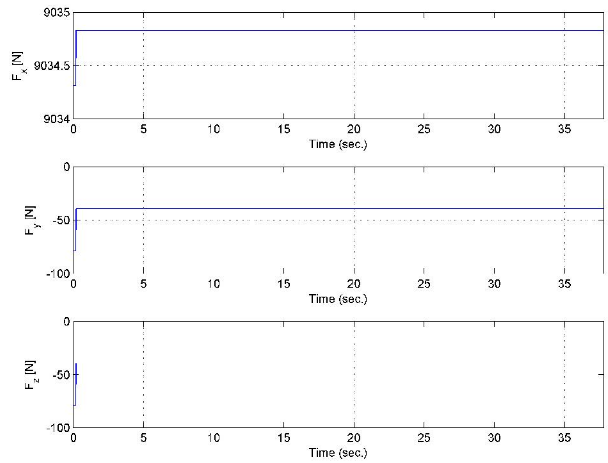

Fig. 9. The three-axis thrust vectors with disturbances.

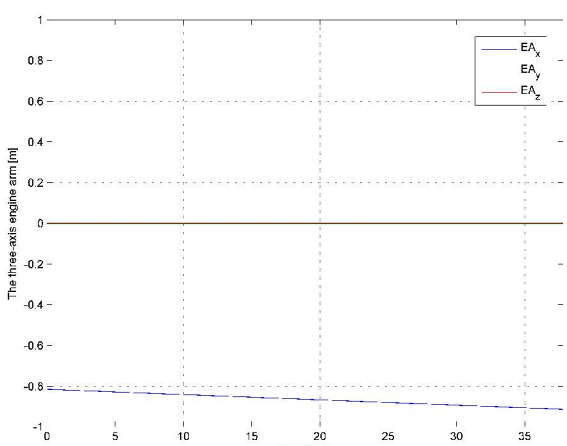

Fig. 7. The three-axis EA.

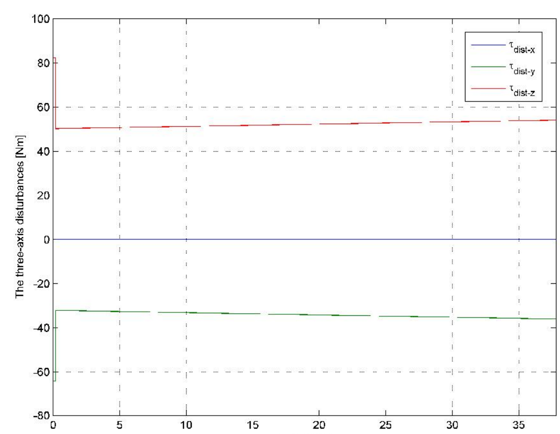

Fig. 10. The three-axis torques disturbances.

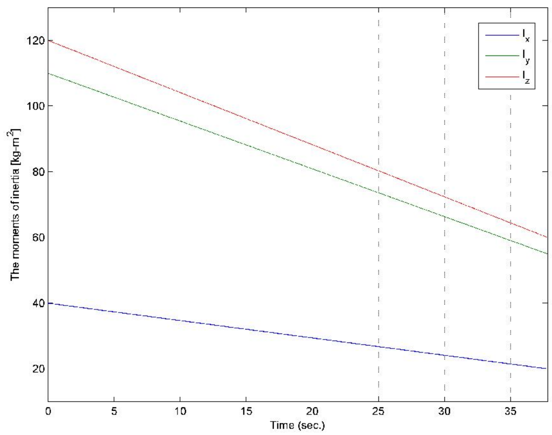

Fig. 11. The moments of the inertial of the spacecraft.

Table 4. The verification of the proposed control approach w. r. t. the corresponding benchmarks.

The approach titles	Maximum three-axis RAE in steady state (°)	Maximum three-axis AER in steady state (°/sec.)	Trajectory convergenc e time (sec.)	Enabling the thrusters (Number/sec.)
The proposed TAAC approach	< 0.50	< 0.05	< 3	< 500
The Yang approach [16]	0.80	-	< 2.5	-
The Cai approach [17]	0.70	0.07	< 5	-

5. Conclusion

The contribution of the present research is concentrated to realize an orbital transferring process that is related to the variation of the orbital parameters in the span of burn time. In the same way, these parameters including semi major axis, eccentricity, apogee radius, inclination, argument of perigee and right ascension of ascending node should first be calculated in the process of 3D orbital maneuvering to present steering angles in the form of quantic polynomials. A wide range of variations in spacecraft to represent the real space environments is focused. The control approach proposed here is organized to deal two sets of low-high thrusters, while pulse-width pulse-frequency modulator as well as control allocation are employed to track three-axis referenced rotational commands, which are directly related to steering angles.

6. References

[1] Curtis, Howard D. 2010. Orbital Mechanics For Engineering Students. 2nd ed. Oxford: Elsevier Butterworth-Heinemann.

[2] An-Min Zou, Kumar, K.D., Zeng-Guang Hou, Xi Liu, Finite-Time Attitude Tracking Control for Spacecraft Using Terminal Sliding Mode and Chebyshev Neural Network, IEEE Transactions on Systems, Man, and Cybernetics, Part B, Volume: 41 Issue: 4, 2011 , Pages 950 – 963.

[3] Chit Hong Yam, Di Lorenzo, D. , Izzo, D., Constrained global optimization of low-thrust interplanetary trajectories, IEEE Congress on Evolutionary Computation (CEC), 2010, Pages 1-7.

[4] Jiang Xiao-yong, Zhang Hong-bo, Tang Guo-jian, A novel low-thrust trajectory optimization approach based on virtual gravitational body, Chinese Automation Congress (CAC), 2013, Pages 295-299.

[5] Jiang Xiao-yong, Lian Yi-jun, Zhang Hong-bo, Tang Guo-jian, A multi-impulse extended method for low-thrust trajectory optimization, International Conference on Recent Advances in Space Technologies (RAST), 2013, Pages 36-368.

[6] Bando, M., Yamakawa, H., Low-thrust trajectory optimization using second-order generating functions, Proceedings of SICE Annual Conference, 2010, Pages 804-810.

[7] Ran Dai, Maximoff, J., Mesbahi, M., Optimal Trajectory Generation for Establishing Connectivity in Proximity Networks, IEEE Transactions on Aerospace and Electronic Systems, 2013, Volume 49, Issue 3, Pages 1968-1981.

[8] Bailing Tian, Wenru Fan, Rui Su, Qun Zong, Real-Time Trajectory and Attitude Coordination Control for Reusable Launch Vehicle in Reentry Phase, IEEE Transactions on Industrial Electronics, 2015, Volume 62, Issue 3, Pages 1639-1650.

[9] J. K. Pieper, Error analysis of direction cosines and quaternion parameters techniques for aircraft attitude determination, IEEE Transactions on Aerospace and Electronic Systems, 1998, Vol. 34, Issue 3, Pages 983 – 989.

[10] N. Lovren, J.K. Pieper, A strapdown inertial navigation system for the flat-Earth model, IEEE Transactions on Aerospace and Electronic Systems, 1997, Vol. 33, Issue 1, Pages 214 – 224.

[11] Bing Xiao , Qinglei Hu, Peng Shi, Attitude Stabilization of Spacecrafts Under Actuator Saturation and Partial Loss of Control Effectiveness, IEEE Transactions on Automation and Engineering, 2013, Volume 21 , Issue 6, Pages 2251-2263.

[12] Bing Xiao , Qinglei Hu, Danwei Wang, Eng Kee Poh, Attitude Tracking Control of Rigid Spacecraft With Actuator Misalignment and Fault, IEEE Transactions on Control Systems Technology, 2013, Volume 21 , Issue 6, Pages 2360-2366.

[13] An-Min Zou, Kumar, K.D., Zeng-Guang Hou, Attitude Coordination Control for a Group of Spacecraft Without Velocity Measurements, IEEE Transactions on Control Systems Technology, 2012, Volume 20 , Issue 5, Pages 1160-1174.

[14] A.M. van der Wielen, F.L.M. Delbressine, P.H.J. Schellekens, Overactuation: A solution for the accuracy–throughput speed contradiction in parallel axis positioning systems, Mechanism and Machine Theory, Volume 46, Issue 11, November 2011, Pages 1732-1743

[15] Zhong Zheng, Shenmin Song, Autonomous attitude coordinated control for spacecraft formation with input constraint, model uncertainties, and external disturbances, Chinese Journal of Aeronautics, Volume 27, Issue 3, June 2014, Pages 602-612.

[16] Y. Yang, Spacecraft attitude determination and control: Quaternion based PDLQR method, Annual Reviews in Control, Volume 36, Issue 2, December 2012, Pages 198-219.

[17] He Cai, Jie Huang, The leader-following attitude control of multiple rigid spacecraft systems, Automatica, Volume 50, Issue 4, April 2014, Pages 1109-1115.